8842–8854 *Nucleic Acids Research, 2016, Vol. 44, No. 18* *Published online 27 August 2016*
doi: 10.1093/nar/gkw746

Tumor suppressor protein DAB2IP participates in chromosomal stability maintenance through activating spindle assembly checkpoint and stabilizing kinetochore-microtubule attachments

Lan Yu[1,†], Zeng-Fu Shang[1,2,†], Salim Abdisalaam[1], Kyung-Jong Lee[1], Arun Gupta[1], Jer-Tsong Hsieh[3,4,5], Aroumougame Asaithamby[1], Benjamin P.C. Chen[1,4,*] and Debabrata Saha[1,4,*]

[1]Department of Radiation Oncology, University of Texas Southwestern Medical Center, Dallas, TX 75390, USA, [2]School of Radiation Medicine and Protection, Medical College of Soochow University; Collaborative Innovation Center of Radiation Medicine of Jiangsu Higher Education Institutions, Suzhou, Jiangsu 215123, China, [3]Department of Urology, University of Texas Southwestern Medical Center, Dallas, TX 75390, USA, [4]Simmons Comprehensive Cancer Center, University of Texas Southwestern Medical Center, Dallas, TX 75390, USA and [5]Department of Oncology, National Taiwan University Hospital, National Taiwan University College of Medicine, Taipei 10048, Taiwan

Received February 12, 2016; Revised July 14, 2016; Accepted August 17, 2016

ABSTRACT

Defects in kinetochore-microtubule (KT-MT) attachment and the spindle assembly checkpoint (SAC) during cell division are strongly associated with chromosomal instability (CIN). CIN has been linked to carcinogenesis, metastasis, poor prognosis and resistance to cancer therapy. We previously reported that the DAB2IP is a tumor suppressor, and that loss of DAB2IP is often detected in advanced prostate cancer (PCa) and is indicative of poor prognosis. Here, we report that the loss of DAB2IP results in impaired KT-MT attachment, compromised SAC and aberrant chromosomal segregation. We discovered that DAB2IP directly interacts with Plk1 and its loss inhibits Plk1 kinase activity, thereby impairing Plk1-mediated BubR1 phosphorylation. Loss of DAB2IP decreases the localization of BubR1 at the kinetochore during mitosis progression. In addition, the reconstitution of DAB2IP enhances the sensitivity of PCa cells to microtubule stabilizing drugs (paclitaxel, docetaxel) and Plk1 inhibitor (BI2536). Our findings demonstrate a novel function of DAB2IP in the maintenance of KT-MT structure and SAC regulation during mitosis which is essential for chromosomal stability.

INTRODUCTION

DAB2IP, also known as apoptosis signal-regulating kinase 1-interacting protein-1 (AIP1), is a Ras-GTPase activating factor and a tumor suppressor. It is often downregulated by epigenetic silencing in many advanced cancer types (1–5). DAB2IP is a scaffold protein that bridges both survival and death signaling cascades to maintain a state of cellular homeostasis through suppression of the PI3K-Akt pathway and enhancement of ASK1-JNK-mediated apoptosis (6). Recent studies have demonstrated that the loss of DAB2IP in castration-resistant prostate cancer can enhance androgen receptor signaling (7). Moreover, the tumor suppressor function of DAB2IP relies on its ability to prevent epithelial-mesenchymal transition through the inhibition of the Ras-PI3K-Akt and the Ras-NFκB signaling pathways (8,9). Loss of DAB2IP is often detected among the high-risk PCa patients and this phenomenon correlates with the relapse of Prostate-specific antigen (PSA) after definitive external beam radiation therapy (10,11). These studies provide evidence for the tumor suppressive role of DAB2IP. Here, we further identify a new function of DAB2IP in suppressing chromosomal instability through modulating and strengthening spindle assembly checkpoint (SAC) regulation.

Both chromosomal instability and consequent aneuploidy (the 'state' of the karyotype) have long been associated with multiple aspects of carcinogenesis (12–14). Earlier studies have reported a strong correlation between chro-

*To whom corespondence should be addressed. Tel: +1 214 648 7750; Fax: +1 214 648 5995; Email: debabrata.saha@utsouthwestern.edu
Correspondence may also be addressed to Benjamin Chen. Tel: +1 214 648 1263; Fax: +1 214 648 5995; Email: benjamin.chen@utsouthwestern.edu
†These authors contributed equally to the work as first authors.

mosomal instability and the defects in SAC (14,15). The SAC is a cell-cycle surveillance system that prevents premature separation of sister chromatids until they are all correctly attached to microtubule fibers originating from opposite poles of the spindle. The bi-orientation is necessary to stabilize the tension across sister kinetochores (KTs) and to silence the SAC sensing mechanism at the KTs (16). The SAC molecules including BubR1, Bub1, Bub3, Mad1 and Mad2 form active complexes at the unattached KTs. BubR1 is the core component of SAC and is involved in recruitment and assembly of other SAC proteins at the KTs (17). Furthermore, BubR1 plays an essential role in the formation of a larger mitotic checkpoint complex with Mad2, Bub3 and Cdc20, ultimately inhibiting the anaphase-promoting complex/cyclosome (APC/C), an E3 ubiquitin ligase complex that facilitates mitotic exit (18).

In addition to its role in SAC signaling and maintenance, BubR1 also participates in the regulation of kinetochore–microtubule (KT–MT) attachment, an essential step towards accurate chromosome segregation and stability (19). Error-free chromosome segregation relies on the formation and subsequent stabilization of the KT–MT interaction, requiring precise control of a set of mitotic factors, including BubR1 and Polo-like kinase 1 (Plk1) (20–22). Plk1 is localized at centrosomes in prophase, and then enriched at the KTs and remains there throughout pro- and metaphase. Plk1 phosphorylates BubR1 at multiple sites which is required for stable KT–MT attachment and chromosome alignment (20–22). Although multiple proteins have been reported for Plk1 activation during mitosis (23,24), further investigations are still needed to identify new regulators of the Plk1–BubR1 axis critically involved in spindle-chromosome interactions and chromosome alignment.

In this study, we described DAB2IP as a positive regulator of the Plk1. DAB2IP directly interacts with Plk1 and facilitates mitotic activation of Plk1. Depletion of DAB2IP in PCa cells significantly compromises mitotic BubR1 phosphorylation resulting in increased levels of misaligned chromosomes during metaphase. We found that DAB2IP deficiency attenuates BubR1 recruitment at the KTs during prometaphase, resulting in compromised SAC activity and aberrant chromosomal segregation. Taken together, our findings report a novel function of DAB2IP in preservation of chromosome stability, highlighting a new mechanism of DAB2IP in PCa pathogenesis.

MATERIALS AND METHODS

Cell lines and treatment

PCa cells C4-2 and PC3 were maintained in T medium (Invitrogen, Carlsbad, CA, USA) containing 5% fetal bovine serum (FBS) (HyClone, Hudson, NH, USA), 10 mM HEPES and 1 mM sodium bicarbonate in a humidified incubator at 37°C with 5% CO2. C4-2 D2 and its control (Neo) cells were generated from C4-2 cells as described previously (8). The HCT116 cell line was purchased from the American Type Culture Collection (ATCC, Manassas, VA, USA) and maintained in Dulbecco's modified Eagle's medium (Invitrogen, Carlsbad, CA, USA) supplemented with 10% FBS (HyClone, Hudson, NH, USA). All cell lines were authenticated through daily monitoring of cell morphology, species verification, growth curve and mycoplasma contamination using MycoAlert PLUS mycoplasma detection kit (Lonza, Allendale, NJ, USA). For mitotic arrest, cells were treated with 50 ng/ml nocodazole (Sigma, St. Louis, MO, USA) or 10 nM paclitaxel (Sigma, St. Louis, MO, USA) for indicated times.

siRNAs and plasmids

Duplex siRNAs were synthesized (Invitrogen, Carlsbad, CA, USA) based on experimentally validated target sequences for DAB2IP siRNA (5′-GGAGCGCAACAG UUACCUGTT-3′), siRNA2 (5′-GGUGAAGGACUUCC UGACATT-3′) or control siRNA (5′-CTGGACTTCC AGAAGAACA-3′) (6). siRNAs were transfected into PC3 cells using Lipofectamine 2000 (Invitrogen, Carlsbad, CA, USA) according to the manufacturer's protocol. HCT116 cells were transfected with pGIPZDAB2IP-lentiviral-shRNAmir and pGIPZ-non-silencing-lentiviral shRNAmir (8) according to the manufacturer's protocol, then the cells were selected by puromycin at concentration of 0.5 μg/ml for 3–4 weeks. For rescue experiments, a DAB2IP construct (mutations underlined: 5′-AGAACGAAATTCTTATTTA-3′) resistant to the siRNA used (5′-GGAGCGCAACAGUUACCUG-3′) was cloned into a pCDNA expression plasmid. Various expression plasmids of DAB2IP were described previously (6).

Antibodies, immunoprecipitation and Glutathione S-Transferase pull down assays

The following primary antibodies were used: rabbit anti-DAB2IP, anti-BubR1 (Bethyl Laboratories, Montgomery, TX, USA); mouse anti-Ku80, rabbit anti-HA, control mouse IgG and rabbit IgG (Santa Cruz Biotechnology, Inc, Dallas, TX, USA); mouse anti-Cyclin B1, rabbit anti-Hsp70, anti-PARP (Cell Signaling Technology Danvers, MA, USA); rabbit anti-phospho–histone H3 (Ser-10) (Millipore, Bellerica, MA, USA); mouse anti-α-tubulin, anti-Flag, rabbit anti-β-actin (Sigma-Aldrich, St. Louis, MO, USA). Secondary antibodies used for immunofluorescence were Alexa Fluor 488 goat anti-mouse IgG, Alexa Fluor 488 goat anti–rabbit IgG, Alexa Fluor 488 goat anti–human IgG, Alexa Fluor 568 goat anti–mouse IgG and Alexa Fluor 568 goat anti–rabbit IgG (Invitrogen Carlsbad, CA, USA).

C4-2 D2 cells were synchronized with nocodazole at prometaphase and cell lysates were incubated with anti-DAB2IP, Plk1 antibodies and protein A/G sepharose overnight. The sepharose beads were washed with lysis buffer three times and resuspended in SDS-PAGE loading buffer for immunoblot analysis using anti-DAB2IP, Plk1 antibodies. For the glutathione S-transferase (GST) pull-down assay, GST–DAB2IP-C′ fusion protein was incubated with glutathione-sepharose beads (GE Healthcare Life Sciences, Piscataway, NJ, USA) and then incubated with recombinant Plk1 or Plk1-(POLO-Box domain) PBD proteins followed by immunoblot analysis.

In vitro kinase assays

For *in vitro* Plk1 kinase assay, immunoprecipitated endogenous Plk1 proteins from C4-2 Neo and C4-2 D2 mitotic cells (incubated with Nocodazol, 50 ng/ml for 16 h) and untreated cells were incubated in Plk1 kinase reaction buffer [20 mM HEPES (pH 7.4), 100 mM KCl, 10 mM $MgCl_2$, 1 mM EDTA, 0.5 mM DTT, 5% glycerol, 10 μM ATP and 0.17 μM γ-32P ATP] with recombinant GST-Cdc25C as substrates. The reaction was incubated for 30 min at 30°C and stopped by adding sodium dodecyl sulfate (SDS) sample buffer. After kinase reaction, samples were subject to SDS-polyacrylamide gel electrophoresis analysis. Incorporation of ^{32}P was analyzed by Typhoon 9410 Imager (GE Healthcare Life Sciences) (25).

Immunofluorescence and live cell imaging

For immunofluorescence analysis, transfected and/or drug-treated cells were plated on 35-mm dishes with coverslips, fixed in 4% paraformaldehyde/PBS for 30 min, permeabilized in 0.5% Triton X-100/PBS for 15 min, and blocked in 5% bovine serum albumin for 30 min. The samples were incubated with anti-α-tubulin (1:1000) and anti-crest (1:2000) antibodies for 3 h, washed three times in phosphate buffered saline (PBS) (10 min each) and incubated with rhodamine red-conjugated goat anti-mouse secondary antibodies (1:1000) for 1 h. The cells were washed in PBS three times (10 min each) and mounted using VECTASHIELD with 4′, 6-diamidino-2-phenylindole (DAPI) (Vector Laboratories, Burlingame, CA, USA). Images were taken under a fluorescence microscope (Axio Imager M2, Carl Zeiss, Thornwood, NY, USA) with AxioVision SE64 Rel.4.8 software (Carl Zeiss, Thornwood, NY, USA). To quantify interkinetochore distances, all images were acquired as Z-stack with 0.4 μm spacing using a 63 X objective. At least 200 kinetochores (>5 cells) were used.

For live-cell imaging, the stable HeLa cell line expressing GFP-H2B was used. Following transfection of siRNAs (control or siDAB2IP), cells were placed on a humidified chamber maintained at 37°C with 5% CO_2. Live-cell imaging was conducted using either a Zeiss LSM510 confocal microscope with a 63X objective or In Cell Analyzer with 60X objective. Cells were followed for 10–12 h, and images were captured at 10 min intervals as specified in the movie legends.

Chromosome spread assays

HCT116 and primary mouse embryonic fibroblasts (MEFs) cells were treated with 100 ng/ml colcemid (Irvine Scientific, Santa Ana, CA, USA) for 6 h. Cells were collected and hypotonically swollen in pre-warmed 75 mM KCl for 13 min at 37°C. Cells were fixed in freshly made Carnoys fixative solution (methanol: acetic acid 3:1) with 2–3 times changes of the fixative. Cells were dropped onto warmed glass slides and dried overnight. Slides were stained with 5% Giemsa for 10 min at room temperature, gently rinsed with running water, air dried and mounted. Slides were visualized using a microscope (BX51, Olympus, Tokyo, Japan) and images were recorded with SPOT Advanced software (SPOT Imaging Solutions, Sterling Heights, MI, USA).

The MTT cell proliferation assays

Exponentially growing DAB2IP-proficient and -deficient C4-2 and PC3 cells were transfected with DAB2IP-siRNA and control-siRNA, trypsinized and counted. One thousand cells were seeded per well in 96-well plates. Cells were treated with indicated doses of paclitaxel, docetaxel and BI2536 for 48 h and then assayed for viability using the previously described MTT assay (26).

Statistical analysis

Data are presented as the mean ± SD of at least three independent experiments. The results were tested for significance using the unpaired Student's *t*-test (**$P < 0.01$ and *$P < 0.05$ were considered significant).

RESULTS

The loss of DAB2IP causes aneuploidy and aberrant chromosome segregation

To determine whether loss of tumor suppressor protein DAB2IP correlated with chromosomal instability, we first analyzed the chromosome number in karyotypically-stable human colon carcinoma HCT116 cell lines. We transfected *DAB2IP* shRNA into HCT116 cells and selected stable subclones with different expression levels of DAB2IP (Figure 1A). The knock down of *DAB2IP* in HCT116 cells resulted in a significant increase of aneuploidy and proportion of aneuploid cells was associated with the degree of DAB2IP depletion (Figure 1A and B). Furthermore, we analyzed whether DAB2IP loss influenced chromosome stability in primary MEFs. Chromosome spreads from two pairs of WT and DAB2IP KO primary MEFs revealed that KO cells exhibited more aneuploidy (Figure 1C). One potential cause of chromosomal instability is improper KT–MT attachments during metaphase which leads to subsequent chromosome lagging in anaphase (27). We then detected aberrant mitosis in PC3 cells transiently transfected with *DAB2IP* siRNA and in C4-2 cells stably expressing *DAB2IP*. We noticed that DAB2IP-expressing C4-2 cells in metaphase possessed aligned chromosomes whereas the majority of DAB2IP-deficient PC3 cells displayed misaligned chromosomes that were separated from the metaphase plates. Consistently, the expression of DAB2IP in C4-2 cells (DAB2IP deficient) caused a significant decrease in lagging chromosomes during anaphase (Figure 1D and E), whereas, depletion of DAB2IP in PC3 (DAB2IP proficient) cells induced lagging chromosome (Figure 1F and G). Most importantly, the aberrant mitosis induced by DAB2IP knockdown was reversed by expressing siRNA-resistant DAB2IP protein.

Therefore, our results suggested a strong correlation between DAB2IP deficiency and aberrant mitotic progression. To further confirm, HeLa cells expressing the H2B–GFP fusion protein were monitored under a video microscope to capture chromosome dynamics during mitotic progression (Figure 2A). Live cell imaging analysis showed that the siRNA-mediated depletion of DAB2IP markedly prolonged the onset of mitosis due to aberrant mitotic progression (Figure 2B). We observed significant increases of

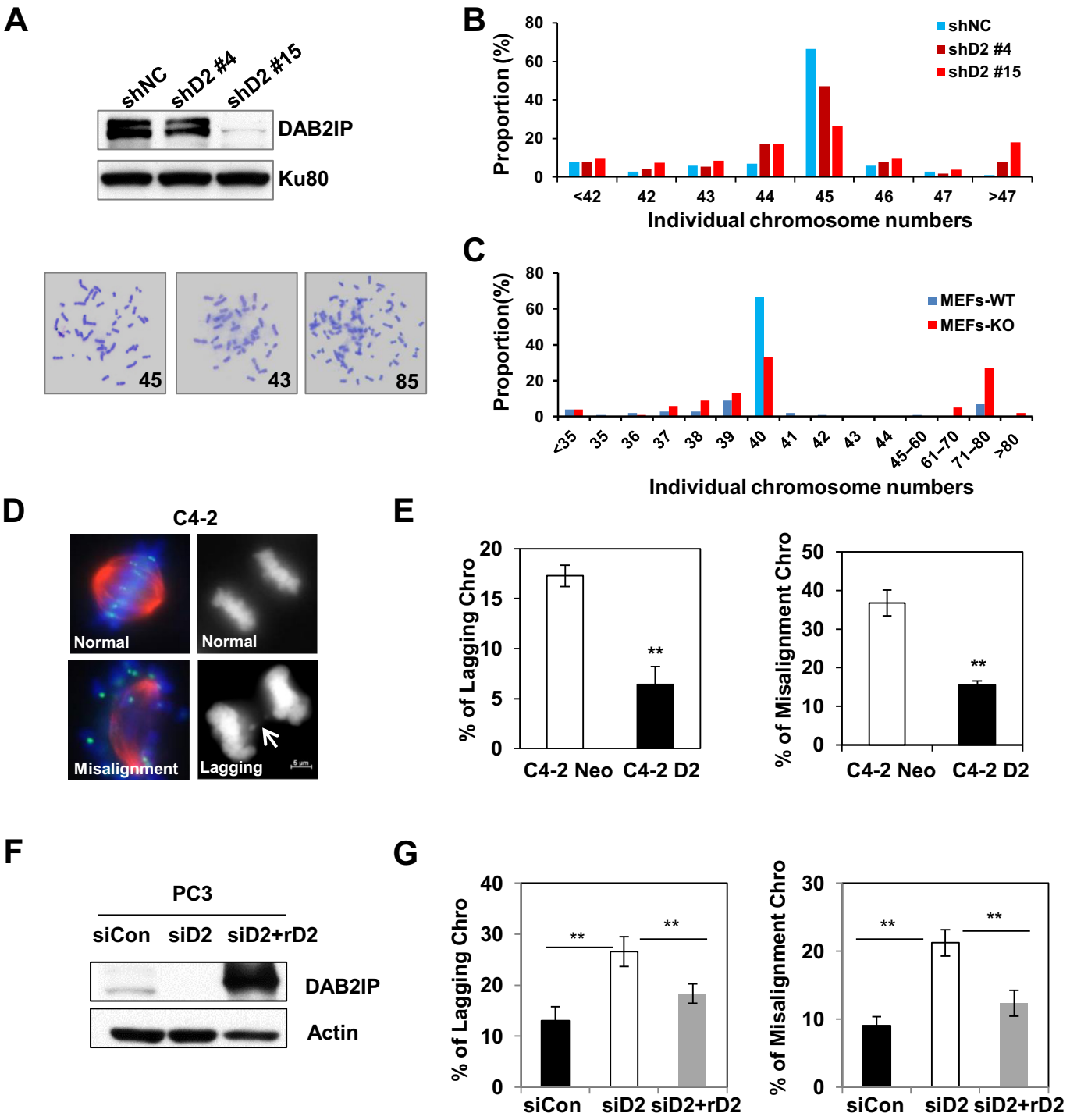

Figure 1. DAB2IP inhibits missegregation and aneuploidy. (**A**) Upper panel: Immunoblot analysis of the shRNA-mediated suppression of DAB2IP protein in HCT116 cells. HCT116 shD2 #4 and #15 are two stable subclones. Lower panel: Representative images of diploidy and aneuploidy chromosome spread in HCT116 cells. (**B**) Chromosome numbers from individual metaphase spreads of control- and DAB2IP-shRNA transfected HCT116 cells. (**C**) Chromosome numbers from individual metaphase spreads of DAB2IP knockout and wild type primary MEFs. (**D**) Representative images of normal and missegragation (lagging) or misaliged chromosomes in C4-2. Cells were stained with anti-α-tubulin and anti-crest antibodies. Scale bar, 5 μm. (**E**) Proportion of cells with chromosome-missegregation and misaligment in C4-2 Neo and C4-2 D2 cells are presented as the mean and SD from three independent experiments (**$P < 0.01$ as compared with control cells). (**F**) Immunoblot analysis of the siRNA-mediated DAB2IP suppression and overexpression of siRNA-resistant DAB2IP (rD2) construct in PC3 cells. (**G**) Overexpression of siRNA-resistant DAB2IP rescued the mitotic phenotypes in PC3 siD2 cells. The results are mean and SD from three independent experiments.

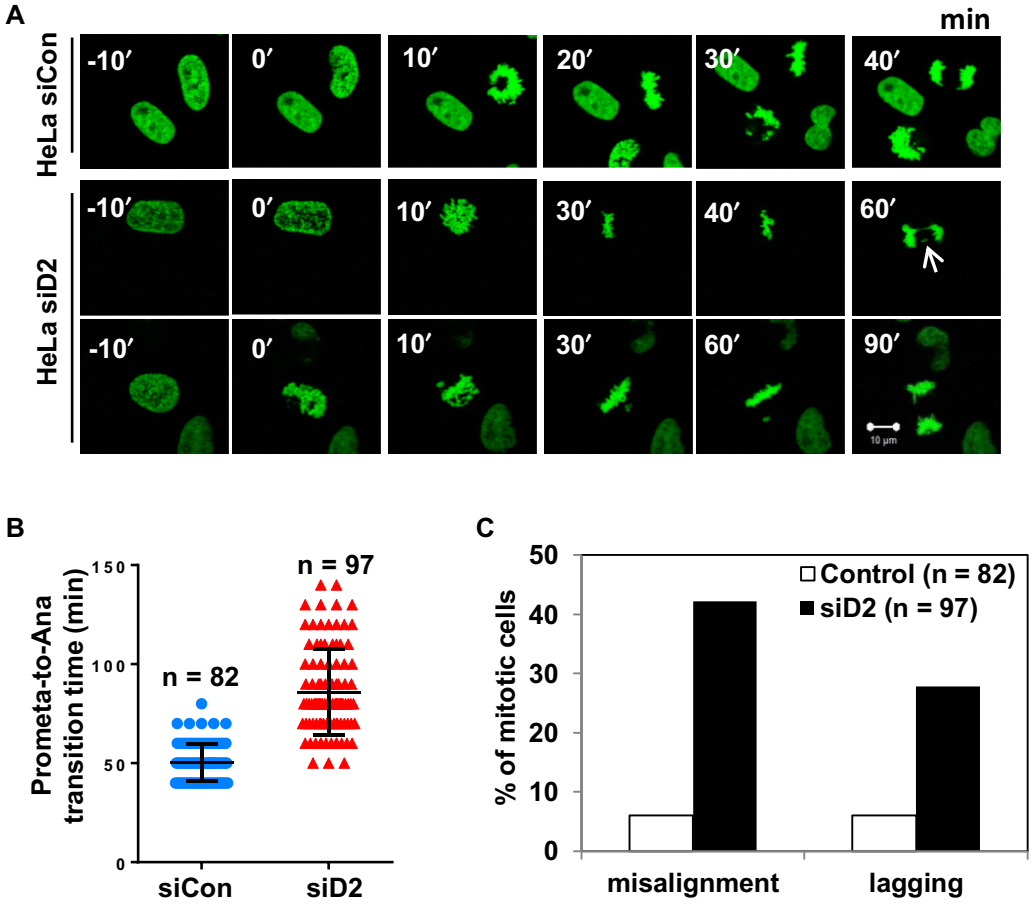

Figure 2. Loss of DAB2IP delays mitosis progression. (**A**) HeLa GFP-H2B cells were transfected with control siRNA or DAB2IP siRNA before live cell image recording. Representative images of mitotic progression are shown 48 h after siRNA transfection (Supplementary movies 1–3). Arrows indicate representative misaligned and lagging chromosomes under evaluation. Scale bar, 10 μm. (**B**) The time elapsed between beginning of chromosome condensation onset to anaphase onset in control siRNA (n = 82) and DAB2IP siRNA cells (n = 97) treated as in A. All cells were counted from four independent experiments. (**C**) Mitotic cells with misaligned chromosomes and lagging chromosomes were quantified in cells treated as in A.

misaligned and lagging chromosomes in DAB2IP-deficient HeLa cells when compared with control HeLa cells (Figure 2C).

The depletion of DAB2IP compromises the stability of KT–MT attachments

The generation of misaligned chromosomes may be due to a dysregulation of the KT–MT interaction. To determine whether DAB2IP contributes to stabilizing the KT–MT attachment, DAB2IP-proficient and -deficient PCa cells were treated with ice-cold medium for different periods of time to weaken the microtubule fibers. Immunofluorescence staining was conducted on cells to count the KT–MTs status (all KT–MTs intact, few short KT–MTs or no KT–MTs) as previously described (28). DAB2IP-expressing C4-2 D2 cells were more cold-resistant compared to C4-2 Neo cells (Figure 3A and B). Many 'few short KT-MTs' persisted in C4-2 D2 cells even 20 min after cold treatment, whereas, C4-2 Neo cells had no visible KT–MT at the same time point. DAB2IP-proficient PC3 cells exhibited a more stable KT–MT interaction when compared with C4-2 cells, and depletion of DAB2IP using siRNA significantly decreased the percentage of cells with stable KT–MTs. Unstable KT-MT attachment reduces the tension of the microtubules across sister KTs at metaphase (29,30). To further prove the role of DAB2IP in establishing KT–MT attachment, the inter-KT distance was measured in DAB2IP-deficeint and proficient PCa cells. In C4-2 Neo cells, the inter-KT distance between sister KTs was 1.00 ± 0.09 μM at metaphase, whereas C4-2 D2 cells increased to 1.21 ± 0.13μM (Figure 3C). Similarly, PC3 and DAB2IP-depleted PC3 cells have 1.62 ± 0.14 μM and 1.32 ± 0.12 μM inter-KT distance, respectively (Figure 3D). These results suggest that the presence of DAB2IP regulates KT–MT interaction.

DAB2IP deficiency impairs mitotic arrest induced by microtubule damage drugs

The premature segregation of chromosomes along with a weakened SAC increases the frequency of aneuploid cells (31). To examine whether DAB2IP is involved on SAC, DAB2IP proficient and deficient PCa cells were treated with nocodazole that destabilizes microtubules and induces mi-

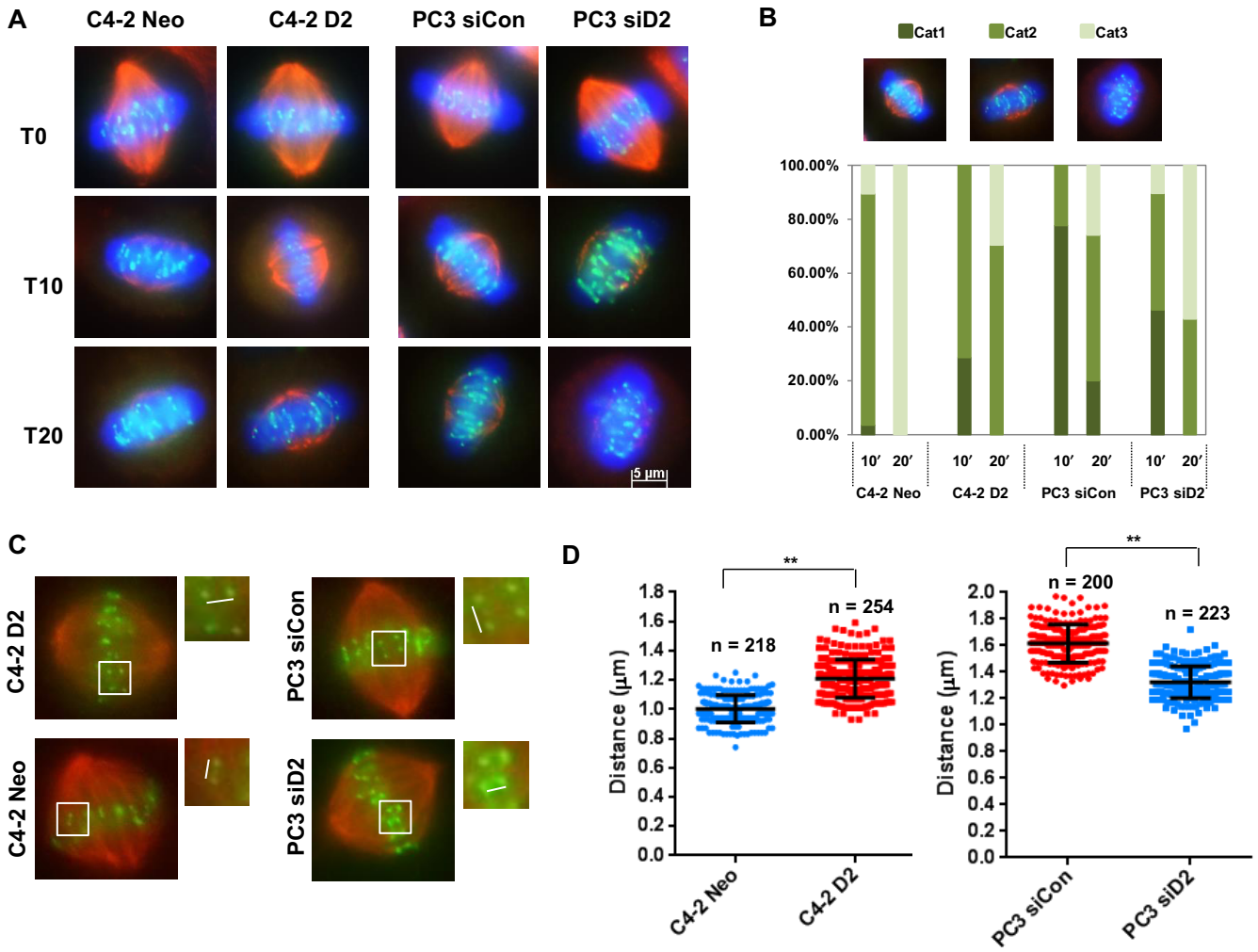

Figure 3. Loss of DAB2IP decreases KT–MT stability. (**A**) C4-2 Neo, C4-2 D2 and siControl, siDAB2IP transfected PC3 cells were treated with ice-cold medium for 10 and 20 min followed by MG132 treatment for 2 h and stained with anti-CREST (kinetochores; green) and anti-α-tubulin antibodies (MTs; red). Scale bar, 5 μm. (**B**) Stable KT–MTs were quantified in cold-treated cells. The bar graph indicates the percentage of cells with all KT–MTs intact (Cat1), possessing few short KT–MTs remaining (Cat2) or possessing no KT–MTs (Cat3). (**C**) Inter-distance of paired KT–MTs at metaphase in C4-2 and PC3 cells. (**D**) Average inter-kinetochore distances of C4-2 and PC3 cells. To quantify inter-kinetochore distances, all images were acquired as Z-stack with 0.4 μm spacing using a 63 X objective. At least 200 kinetochores (>5 cells) were analyzed in each cell lines. Error bars represent SD (**$P < 0.01$ as compared with control cells).

totic arrest. The mitotic index was determined by staining with a pH3-specific antibody and propidium iodide. C4-2 D2 cells exhibited a higher mitotic index compared to C4-2 Neo cells upon nocodazole treatment (Figure 4A and B). Consistent with the FACS analysis, the expression levels of mitosis specific cyclin B1 in C4-2 D2 cells was much higher compare to control C4-2 cells (Figure 4C). In addition, DAB2IP depleted PC3 cells and DAB2IP-knockout MEFs exhibited reduced mitotic index by nocodazole treatment when compared to DAB2IP positive cells (Figure 4D, E and Supplementary Figure S1). Interestingly, when analyzing the mitotic progression in single cell, we observed the time for mitosis is extended in DAB2IP deficient cells that can be attributed to the generation of aberrant mitotic cells. However, we noticed a decrease of mitotic index in DAB2P-depleted cells, indicating DAB2IP might also play an important role in regulating G2-M transition. Altogether, these experiments indicated that expression of DAB2IP induced a strong mitotic spindle checkpoint, through which DAB2IP blocked premature chromosome segregation and aneuploidy.

DA2BIP enhances kinetochore localization and mitotic phosphorylation of BubR1

Our results revealed a novel role of DAB2IP in the important mitotic events such as SAC maintenance and proper chromosome–spindle interaction. Mitotic BubR1 kinase is one of the key regulators of these processes during mitotic progression and the dysregulation of BubR1 inhibits both SAC activity and chromosome congression in the metaphase plate (32). To determine whether DAB2IP participates in mitotic regulation through the BubR1 pathway, we examined the role of DAB2IP on BubR1 localization at

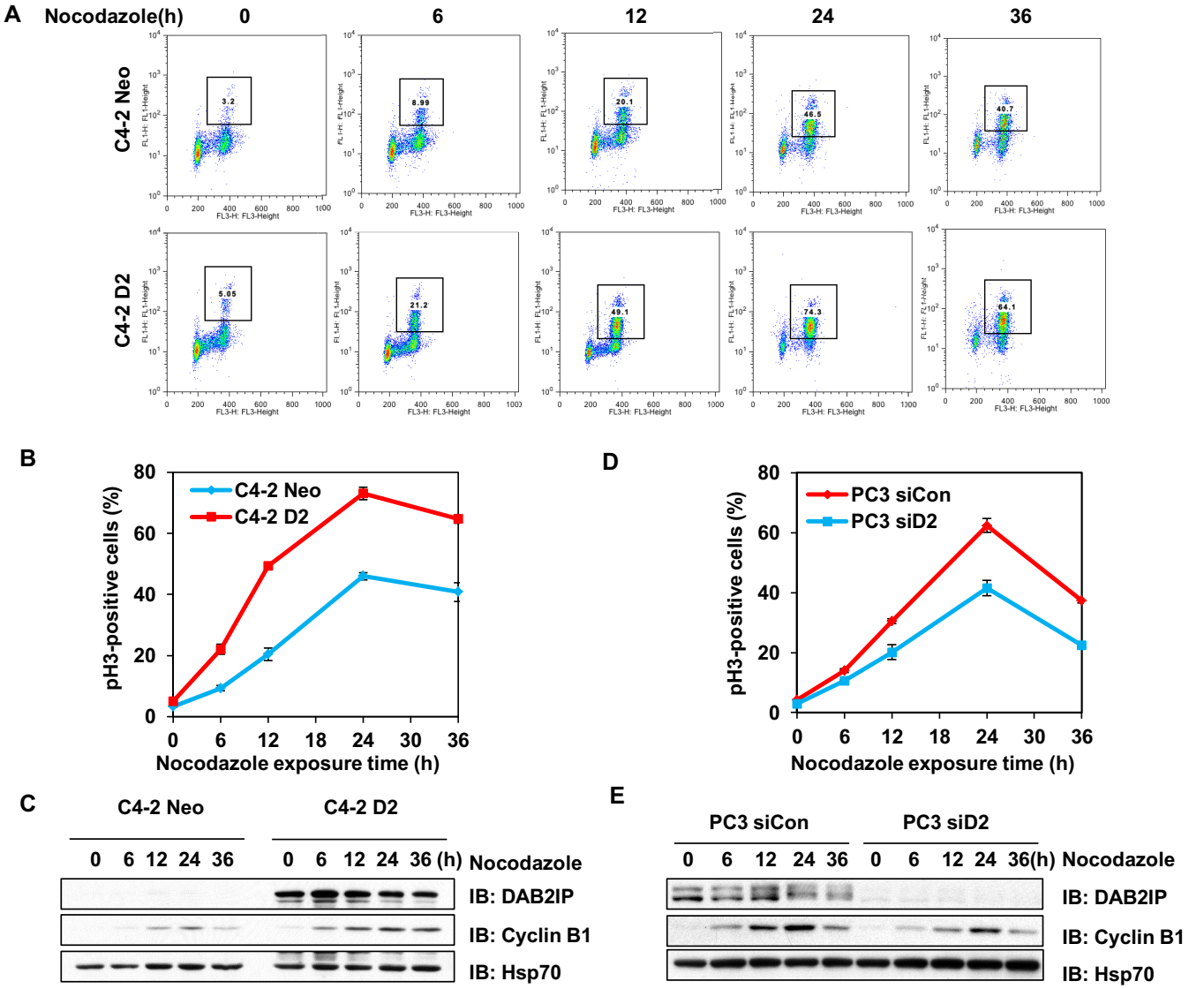

Figure 4. DAB2IP maintains a robust spindle assembly checkpoint. (**A**) C4-2 Neo/D2 cells and PC3 siCon/siD2 cells were treated with 50 ng/ml nocodazole for different times. Cells were collected and fixed at the indicated time and the percentage of pH3-positive cells were determined by flow cytometry. (**B** and **D**) Quantification of mitotic index in C4-2 Neo/D2 and PC3 siCon/siD2 cells under similar experimental conditions those mentioned in A (from 3 independent experiments). (**C** and **E**) Expression levels of DAB2IP, cyclin B1 and HSP70 were analyzed by immunoblot analysis.

the KT. As usual, BubR1 was strongly visible at the KTs in PC3 cells, but the depletion of DAB2IP dramatically diminished the presence of BubR1 at the KTs (Figure 5A and B). A similar decrease of BubR1 at the KTs was also observed in DAB2IP knockdown DU145 cells (Supplementary Figure S2A). In contrast, reconstituting DAB2IP in C4-2 cells significantly restored BubR1 level at the KTs (Figure 5C). In addition to KT localization, phosphorylation at multiple sites of BubR1 may also contribute to its function in KT–MT attachment and proper chromosome alignment (32). DAB2IP-proficient and -deficient PCa cells were treated with nocodazole to block cell cycle progression at mitosis. Immunoblot was performed to detect the slowly migrating band of BubR1, representing its phosphorylated form (33). The knock down of DAB2IP significantly inhibited mitotic BubR1 phosphorylation in PC3 cells (Figure 5D), whereas its expression in C4-2 cells facilitated BubR1 phosphorylation during mitosis (Figure 5E). A similar phenomenon was shown in DU145 cells (Supplementary Figure S2B). We reintroduced siRNA-resistant DAB2IP into DAB2IP knockdown PC3 cells, and successfully restored the mitotic phosphorylation of Plk1 and BubR1 (Supplementary Figure S3). These results indicate that DAB2IP may recruit BubR1 to the kinetochore and facilitate BubR1 phosphorylation at the same time.

DAB2IP interacts with Plk1 and promotes Plk1 activation

Plk1 phosphorylates BubR1 and the Plk1-dependent phosphorylation of BubR1 is involved in KT–MT attachment and chromosome congression (20,21). We assessed the mitotic induction of Plk1 autophosphorylation at Thr210 in DAB2IP-proficient and -deficient PCa cells. We found that

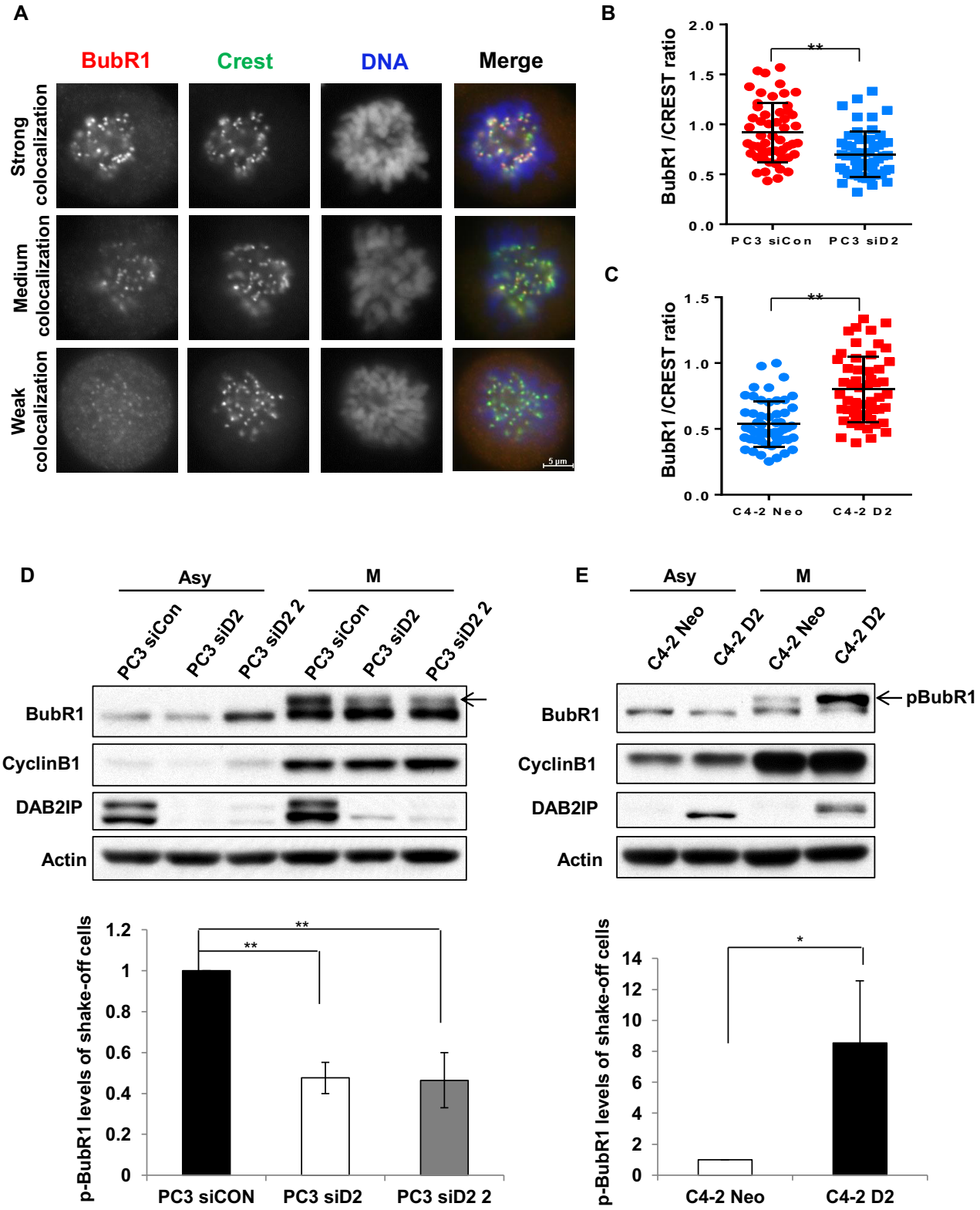

Figure 5. Decreased kinetochore localization and phosphorylation of BubR1 in DAB2IP deficient PCa cells. (**A**) Representative images of strong, medium and weak BubR1 colocalization with kinetochores (CREST). Forty-eight hours after transfection with control or DAB2IP siRNA, PC3 cells were fixed and immunostained with anti-BubR1 and CREST antibodies. Colocalization of BubR1 with CREST antibody-stained structures (kinetochores) was detected under a fluorescence microscope. Scale bar, 5 μm. (**B** and **C**) Quantification of BubR1 levels (normalized by CREST) on prometaphase kinetochores in paired (B) PC3 and (C) C4-2 cells. (n = 54 cells) (**$P < 0.01$ as compared with control cells). (**D**) Paired PC3 and (**E**) C4-2 cells were treated with nocodazole (50 ng/ml) for 16 h. Mitotic and untreated cells were analyzed by immunoblotting with anti-BubR1, anti-CyclinB1, anti-DAB2IP and anti-Actin antibodies. Error bars represent SD. The results represented are from 3 independent experiments. Asy, asynchronized. (**$P < 0.01$ and *$P < 0.05$ as compared with control cells).

the levels of mitotic Plk1 phosphorylation at Thr210 were consistently elevated in several DAB2IP proficient PCa cells (Figure 6A and B). To further validate the function of DAB2IP on Plk1 activity, endogenous Plk1 were immunoprecipitated from C4-2 D2 and C4-2 Neo cells for *in vitro* kinase assay using Cdc25C as the substrate. Our result revealed that Plk1-mediated Cdc25C phosphorylation was markedly enhanced in C4-2 D2 when compared to C4-2 Neo, suggesting that DAB2IP promotes activation of Plk1 (Figure 6C).

We further tested whether DAB2IP could interact with Plk1 during mitosis. Mitotic C4-2 D2 cells were enriched using nocodazole treatment and were harvested by mitotic shake off. Synchronized cell lysates were subjected to co-IP with anti-DAB2IP or anti-Plk1 antibodies. Consistently, DAB2IP and Plk1 association was detected in reciprocal co-IP analyses (Figure 6D). To further characterize DAB2IP and Plk1 interactions, Flag-tagged DAB2IP expression constructs, which cover various regions of DAB2IP, were co-transfected with HA-Plk1 in 293T cells followed by co-IP using an anti-Flag antibody. Our data indicated that the CPR domain of DAB2IP interacts with Plk1 (Figure 6E). To further confirm the direct protein–protein interaction between DAB2IP and Plk1, the full length His-tagged Plk1 was expressed and purified from *E.coli* and was subjected to a GST pull-down experiment using GST alone or GST fused with DAB2IP C-terminal domain. His-Plk1 could directly interact with DAB2IP C-terminal domain (Figure 6F). This interaction is mediated by the polo-box domain of Plk1 as it could also interact with DAB2IP-C' *in vitro* (Figure 6F).

DAB2IP deficient prostate cancer cells are resistant to microtubule-stabilizing drugs and Plk1 inhibitor

Microtubule-stabilizing agents have been extensively used in the treatment of solid tumors including prostate cancer (34,35). However, resistance to chemotherapy can develop leading to poor clinical outcomes for patients (36,37). These anti-mitotic drugs, such as paclitaxel, inhibit cancer cells by SAC mediated mitotic arrest and catastrophe (38). Cancer cells with weakened SAC function were found to be resistant to these microtubule inhibitors (39). Consistently, we found that DAB2IP expression increased paclitaxel-induced mitotic arrest in C4-2 D2 and PC3 siCon cells as compared to DAB2IP deficient cells (Figure 7A and B). In addition, we demonstrated that DAB2IP-proficient PCa cells exhibit higher sensitivity toward paclitaxel or docetaxel treatment as compare to DAB2IP-deficient cells (Figure 7C and D). Multiple studies have revealed that protracted mitotic arrest plays a pivotal role in post mitotic cell death (40). We noticed that PARP-1 cleavage was greater in C4-2 D2 cells when compared to C4-2 Neo cells in response to paclitaxel (Figure 7F). Similar results were also observed in HeLa cells (Supplementary Figure S4).

Since our results clearly showed that DAB2IP promote Plk1 activity, DAB2IP-proficient tumors might exhibit an addiction to Plk1 kinase and hence demonstrate a hypersensitivity to Plk1 inhibitor. Consistent with this notion, DAB2IP-proficient PCa cells were found to be highly sensitive to the specific Plk1 inhibitor BI2536 (Figure 7E).

DISCUSSION

DAB2IP is a tumor suppressor protein that negatively modulates multiple oncogenic signaling pathways (6,8,41). In this study, we revealed a novel role of DAB2IP in regulating chromosome–spindle interaction (Figure 3) and mitotic SAC (Figure 4). The loss of DAB2IP disrupted KT–MT attachment and inhibited SAC activity, both of which are leading factors for chromosomal instability and tumorigenesis. Hence, our current study provides a unique molecular mechanism, in which DAB2IP functions as a gate keeper of chromosomal stability, ensuring proper chromosome congression and segregation during mitosis.

Plk1 is considered as a central regulator of mitotic progression from mitotic entry to exit (42). Our findings confirmed that DAB2IP facilitates mitotic checkpoints and chromosome congression via Plk1 activation. Plk1 localizes on unattached KTs and plays pivotal role in promoting MT–KT interaction and regulation of SAC (42). The activation process of Plk1 initiates after the interaction of its C-terminal polo-box domain with a series of targets proteins, followed by the release of its N-terminal kinase domain (42). We showed that DAB2IP directly interacts with the PBD domain of Plk1 and promoting its activation (Figure 6). Plk1 or other kinases primarily phosphorylate substrates to create a docking site for the PBD domain of Plk1 and then recruit more Plk1 to enhance its concentration and activity. The results of this study provide an opportunity to further explore whether DAB2IP is a target of Plk1 kinase or other mitotic kinases.

Activated Plk1 phosphorylates a set of kinetochore proteins, such as Mps1. Phosphorylated Mps1 facilitates its catalytic activity and enhances kinetochores localization of SAC components such as Mad1, Mad2, Bub3 and BubR1 (43). As mentioned earlier, BubR1 is a core component of the mitotic checkpoint complex (17). The loss of BubR1 localization at the kinetochore compromises the mitotic checkpoint resulting in delaying anaphase onset (32). We showed that, DAB2IP positively regulates BubR1 kinetochore localization during mitosis (Figure 5). Therefore, by comparing the roles of BubR1 in SAC, we believe that the presence of DAB2IP strengthens SAC in response to microtubule-damaging agents such as nocodazole (Figure 4). Furthermore, Plk1 can also directly phosphorylate BubR1. This Plk1-mediated phosphorylation of BubR1 is required for the generation of 3F3/2 epitope, which is associated with intra-KT tension (44). In addition, Plk1-mediated BubR1 phosphorylation is also involved in stabilizing KT–MT attachment and regulating chromosome congression (20,21). The contribution of mitotic phosphorylation of BubR1 by Plk1 to KT–MT attachments has been unclear until recently report from Kops *et al.* where they reported KARD domain of BubR1 is the Plk1-mediated phosphorylation sites and is required for interaction with PP2A-B56α. They also reported this interaction is necessary to harness the Aurora B activity on the outer KTs to stabilize KT–MT interaction and facilitate chromosome alignment in metaphase (20). Our data showed that DAB2IP promotes mitotic phosphorylation of BubR1 and also helps to stabilize KT–MT attachment (Figure 3). A number of outstanding mechanisms should be studied fur-

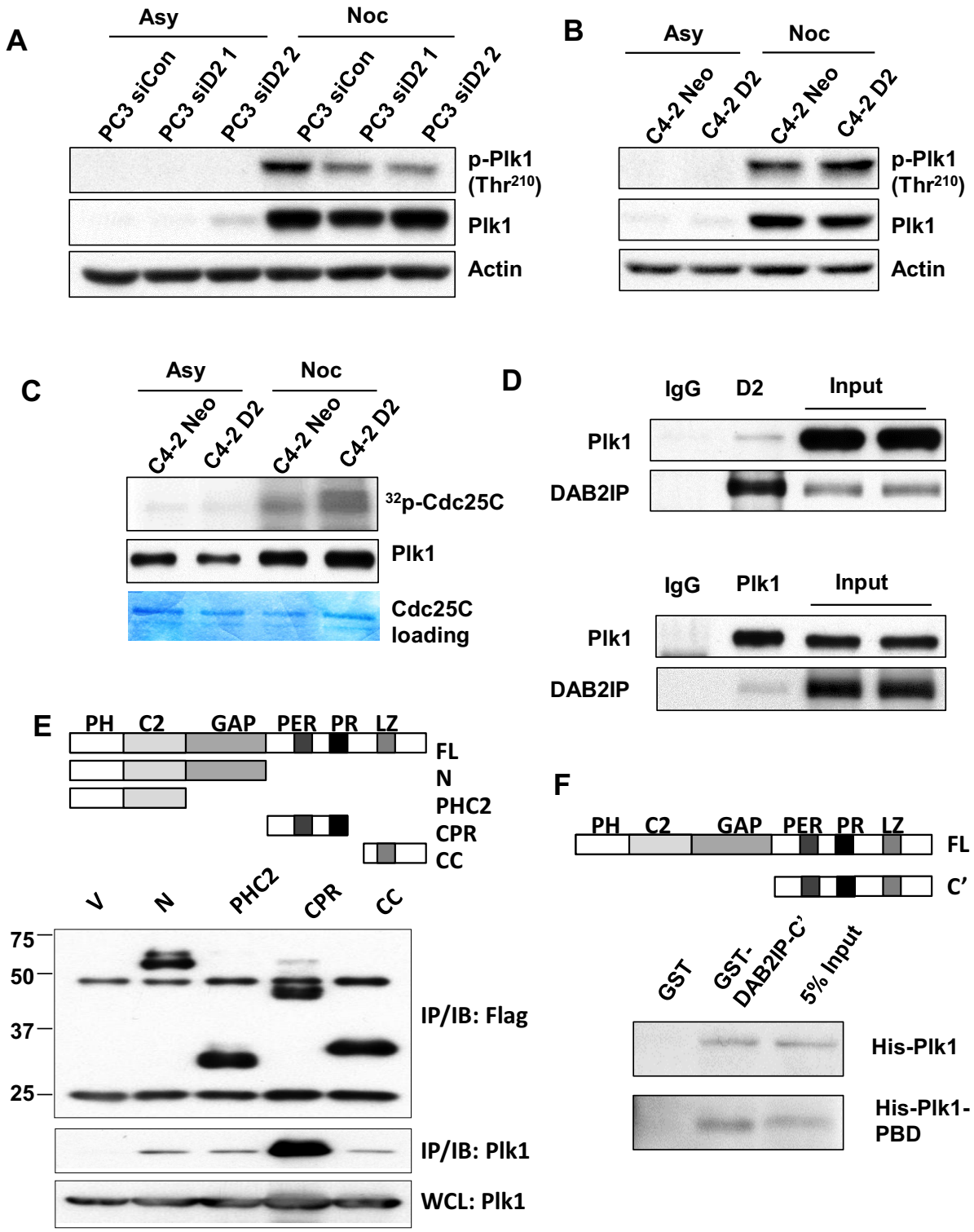

Figure 6. DAB2IP interacts with Plk1 and promotes Plk1 activity. (**A**) Paired PC3 and (**B**) C4-2 cells were treated with nocodazole (50 ng/ml) for 16 h. Mitotic cells and untreated cells were analyzed by immunoblotting with anti- phospho-Plk1 (Thr210), anti-Plk1 and anti-Actin antibodies. (**C**) Mitotic and untreated C4-2 Neo and C4-2 D2 cells were analyzed for Plk1 activity by the Plk1 kinase assay using GST-Cdc25C as the substrate. Phosphorylation of GST-Cdc25C was visualized by autoradiography. Immunoblot analysis of Plk1 showed similar levels of Plk1 in the kinase assay. (**D**) C4-2 D2 cells were synchronized with nocodazole (50 ng/ml) for 16 h and mitotic cells were collected by shake off. Mitotic cell lysates were immunoprecipitated with anti-DAB2IP, anti-Plk1 antibodies or rabbit IgG followed by immunoblot analysis to detect DAB2IP and Plk1 levels. (**E**) Top: Schema of the truncated domains of DAB2IP. Bottom: Various cDNA constructs of DAB2IP truncations were co-transfected with HA-Plk1 into 293T cells and immunoprecipitated using anti-Flag antibody; HA signal was examined by Western blotting. (**F**) Direct protein–protein interaction between DAB2IP and Plk1. GST fusion proteins carrying C-terminal of DAB2IP was incubated with His-tagged full-length Plk1 or Plk1-PBD domain followed by glutathione agarose pull-down. The bound Plk1 or PBD domain was detected by anti-His antibody.

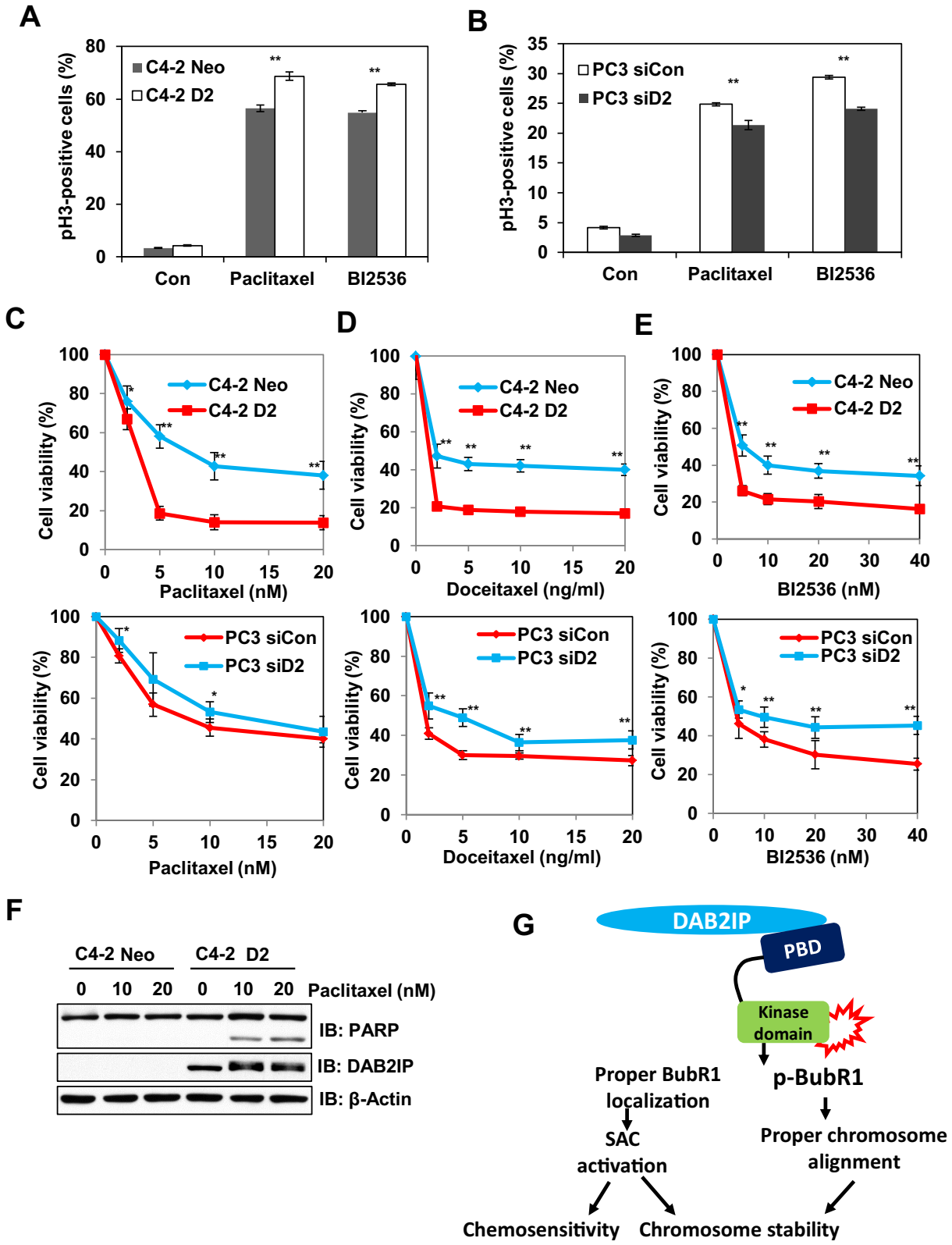

Figure 7. DAB2IP enhances the chemosensitivity of PCa cells with microtubule-stabilizing drugs and Plk1 inhibitor. (**A** and **B**) Paired C4-2 and PC3 cells were treated with paclitaxel, BI2536 and collected at 24 h. Proportion of pH3-positive cells were analyzed by FC. (**C**, **D** and **E**) Paired C4-2 and PC3 cells were exposed to different concentrations of the indicated chemotherapeutic drugs for 48 h and MTT assay was performed. Results obtained from three independent experiments (means ± SD); (**$P < 0.01$ and *$P < 0.05$ as compared with control cells). (**F**) Cells were lysed 24 h after exposure to the indicated concentration of paclitaxel and subjected to immunoblotting with anti-PARP, anti-DAB2IP and anti-Actin antibodies. (**G**) Proposed model of the role of DAB2IP in mitosis regulation.

ther: (i) Whether DAB2IP-induced Plk1 activation participates in mitotic BubR1 phosphorylation and (ii) whether DAB2IP-mediated phosphorylation of BubR1 also facilitates KT-spindle interaction by antagonizing Aurora B activity.

DAB2IP seems to regulate mitotic progression via Plk1 activation. The overexpression of Plk1 has been observed in prostate cancer and its expression levels highly correlate with tumor grade, tumorigenesis and progression (45,46). However, missense mutations of Plk1 were also found in cancer cells (33,47). BubR1 also functions as a barrier to block genomic instability; mutations in BubR1 cause the cancer-susceptible disease Mosaic Variegated Aneuploidy (MVA). Cells derived from MVA patients exhibit an impaired mitotic checkpoint and chromosome misalignment (48), similarly to DAB2IP-deficient cells. The complete loss of SAC is lethal even for tumor cells. However, the partial loss of SAC in concomitance with aberrant chromosome congression is responsible for chromosome missegregation and aneuploidy. We have established the tumor suppressive role of DAB2IP which is partially due to its ability to prevent chromosome missegregation and aneuploidy.

Persistent trapping of cells in mitosis by SAC leads to apoptosis in a Cdk1-dependent manner (49). However, mitotic slippage limits the efficacy of these Cdk inhibitors. Our results demonstrated that the presence of DAB2IP could also increase the sensitivity of PCa cells to paclitaxel or docetaxel (Figure 7) suggesting that the increased cytotoxicity induced by these drugs might stem from the prolonged mitotic block mediated by robust SAC in DAB2IP-proficient PCa cells. In addition, several reports indicated that molecular targeting of Plk1 also blocks cells during mitosis and could be an effective strategy in cancer therapy (50). BI2536 is a specific inhibitor of Plk1 and was tested in a now completed phase II clinical trial of non-small cell lung cancer, pancreatic cancer or hormone-refractory prostate cancer (51). We reported DAB2IP proficient cells showed increased BI2536-induced mitotic arrest (Figure 7).

Based on results, we propose a tentative model for DAB2IP's role in mitosis regulation (Figure 7G). DAB2IP could promote the activation of Plk1 during mitosis, subsequently phosphorylating and facilitating the KT localization of BubR1, and reinforcing SAC activity and chromosome stability. The loss of DAB2IP increases chromosome misalignment and compromises SAC activity ultimately contributing to aneuploidy and subsequent tumorigenesis and chemoresistance.

SUPPLEMENTARY DATA

Supplementary Data are available at NAR Online.

ACKNOWLEDGEMENTS

The authors are grateful to Dr Damiana Chiavolini for editing the manuscript and Dr Brock Sishc for technical help.

FUNDING

National Institute of Health [CA175879 to D.S. and CA166677 to B.P.C.C.]; Department of Defense [W81XWH-11-1-0270 to D.S.]; Cancer Prevention & Research Institute of Texas [RP120670-C3 to D.S.]; National Science Foundation of China [#31500681 and 81472919 to Z.S.]. Funding for open access charge: National Institute of Health [CA175879].
Conflict of interest statement. None declared.

REFERENCES

1. Chen,H., Pong,R.C., Wang,Z. and Hsieh,J.T. (2002) Differential regulation of the human gene DAB2IP in normal and malignant prostatic epithelia: cloning and characterization. *Genomics*, **79**, 573–581.
2. Dote,H., Toyooka,S., Tsukuda,K., Yano,M., Ouchida,M., Doihara,H., Suzuki,M., Chen,H., Hsieh,J.T., Gazdar,A.F. *et al.* (2004) Aberrant promoter methylation in human DAB2 interactive protein (hDAB2IP) gene in breast cancer. *Clin. Cancer Res.*, **10**, 2082–2089.
3. Yano,M., Toyooka,S., Tsukuda,K., Dote,H., Ouchida,M., Hanabata,T., Aoe,M., Date,H., Gazdar,A.F. and Shimizu,N. (2005) Aberrant promoter methylation of human DAB2 interactive protein (hDAB2IP) gene in lung cancers. *Int. J. Cancer*, **113**, 59–66.
4. Shen,Y.J., Kong,Z.L., Wan,F.N., Wang,H.K., Bian,X.J., Gan,H.L., Wang,C.F. and Ye,D.W. (2014) Downregulation of DAB2IP results in cell proliferation and invasion and contributes to unfavorable outcomes in bladder cancer. *Cancer Sci.*, **105**, 704–712.
5. Smits,M., van Rijn,S., Hulleman,E., Biesmans,D., van Vuurden,D.G., Kool,M., Haberler,C., Aronica,E., Vandertop,W.P., Noske,D.P. *et al.* (2012) EZH2-regulated DAB2IP is a medulloblastoma tumor suppressor and a positive marker for survival. *Clin. Cancer Res.*, **18**, 4048–4058.
6. Xie,D., Gore,C., Zhou,J., Pong,R.C., Zhang,H., Yu,L., Vessella,R.L., Min,W. and Hsieh,J.T. (2009) DAB2IP coordinates both PI3K-Akt and ASK1 pathways for cell survival and apoptosis. *Proc. Natl. Acad. Sci. U.S.A.*, **106**, 19878–19883.
7. Wu,K., Liu,J., Tseng,S.F., Gore,C., Ning,Z., Sharifi,N., Fazli,L., Gleave,M., Kapur,P., Xiao,G. *et al.* (2014) The role of DAB2IP in androgen receptor activation during prostate cancer progression. *Oncogene*, **33**, 1954–1963.
8. Xie,D., Gore,C., Liu,J., Pong,R.C., Mason,R., Hao,G., Long,M., Kabbani,W., Yu,L., Zhang,H. *et al.* (2010) Role of DAB2IP in modulating epithelial-to-mesenchymal transition and prostate cancer metastasis. *Proc. Natl. Acad. Sci. U.S.A.*, **107**, 2485–2490.
9. Min,J., Zaslavsky,A., Fedele,G., McLaughlin,S.K., Reczek,E.E., De Raedt,T., Guney,I., Strochlic,D.E., Macconaill,L.E., Beroukhim,R. *et al.* (2010) An oncogene-tumor suppressor cascade drives metastatic prostate cancer by coordinately activating Ras and nuclear factor-kappaB. *Nat. Med.*, **16**, 286–294.
10. Kong,Z., Xie,D., Boike,T., Raghavan,P., Burma,S., Chen,D.J., Habib,A.A., Chakraborty,A., Hsieh,J.T. and Saha,D. (2010) Downregulation of human DAB2IP gene expression in prostate cancer cells results in resistance to ionizing radiation. *Cancer Res.*, **70**, 2829–2839.
11. Yu,L., Tumati,V., Tseng,S.F., Hsu,F.M., Kim,D.N., Hong,D., Hsieh,J.T., Jacobs,C., Kapur,P. and Saha,D. (2012) DAB2IP regulates autophagy in prostate cancer in response to combined treatment of radiation and a DNA-PKcs inhibitor. *Neoplasia*, **14**, 1203–1212.
12. Rajagopalan,H., Nowak,M.A., Vogelstein,B. and Lengauer,C. (2003) The significance of unstable chromosomes in colorectal cancer. *Nat. Rev. Cancer*, **3**, 695–701.
13. McGranahan,N., Burrell,R.A., Endesfelder,D., Novelli,M.R. and Swanton,C. (2012) Cancer chromosomal instability: Therapeutic and diagnostic challenges. *EMBO Rep.*, **13**, 528–538.
14. Gordon,D.J., Resio,B. and Pellman,D. (2012) Causes and consequences of aneuploidy in cancer. *Nat. Rev. Genet.*, **13**, 189–203.
15. Fang,X. and Zhang,P. (2011) Aneuploidy and tumorigenesis. *Semin. Cell Dev. Biol.*, **22**, 595–601.
16. Lara-Gonzalez,P., Westhorpe,F.G. and Taylor,S.S. (2012) The spindle assembly checkpoint. *Curr. Biol.*, **22**, R966–R980.
17. Chen,R.H. (2002) BubR1 is essential for kinetochore localization of other spindle checkpoint proteins and its phosphorylation requires Mad1. *J. Cell Biol.*, **158**, 487–496.

18. Kim,S. and Yu,H. (2011) Mutual regulation between the spindle checkpoint and APC/C. *Semin. Cell Dev. Biol.*, **22**, 551–558.
19. Bakhoum,S.F., Genovese,G. and Compton,D.A. (2009) Deviant kinetochore microtubule dynamics underlie chromosomal instability. *Curr. Biol.*, **19**, 1937–1942.
20. Suijkerbuijk,S.J.E., Vleuge,M., Teixeira,A. and Kops,G.J.P.L. (2012) Integration of kinase and phosphatase activities by BUBR1 ensures formation of stable kinetochore-microtubule attachments. *Dev. Cell*, **23**, 745–755.
21. Elowe,S., Huemmer,S., Uldschmid,A., Li,X. and Nigg,E.A. (2007) Tension-sensitive Plk1 phosphorylation on BubR1 regulates the stability of kinetochore-microtubule interactions. *Genes Dev.*, **21**, 2205–2219.
22. Matsumura,S., Toyoshima,F. and Nishida,E. (2007) Polo-like kinase 1 facilitates chromosome alignment during prometaphase through BubR1. *J. Biol. Chem.*, **282**, 15217–15227.
23. Foley,E.A. and Kapoor,T.M. (2013) Microtubule attachment and spindle assembly checkpoint signalling at the kinetochore. *Nat. Rev. Mol. Cell Biol.*, **14**, 25–37.
24. Kim,J.H., Shim,J., Ji,M.J., Jung,Y., Bong,S.M., Jang,Y.J., Yoon,E.K., Lee,S.J., Kim,K.G., Kim,Y.H. *et al.* (2014) The condensin component NCAPG2 regulates microtubule-kinetochore attachment through recruitment of Polo-like kinase 1 to kinetochores. *Nat. Commun.*, **5**, 4588.
25. Lee,K.J., Shang,Z.F., Lin,Y.F., Sun,J., Morotomi-Yano,K., Saha,D. and Chen,B.P. (2015) The catalytic subunit of DNA-dependent protein kinase coordinates with polo-like kinase 1 to facilitate mitotic entry. *Neoplasia*, **17**, 329–338.
26. van Meerloo,J., Kaspers,G.J. and Cloos,J. (2011) Cell sensitivity assays: The MTT assay. *Methods Mol. Biol.*, **731**, 237–245.
27. Thompson,S.L., Bakhoum,S.F. and Compton,D.A. (2010) Mechanisms of chromosomal instability. *Curr. Biol.*, **20**, R285–R295.
28. Amaro,A.C., Samora,C.P., Holtackers,R., Wang,E., Kingston,I.J., Alonso,M., Lampson,M., McAinsh,A.D. and Meraldi,P. (2010) Molecular control of kinetochore-microtubule dynamics and chromosome oscillations. *Nat. Cell Biol.*, **12**, U319–U342.
29. Draviam,V.M., Shapiro,I., Aldridge,B. and Sorger,P.K. (2006) Misorientation and reduced stretching of aligned sister kinetochores promote chromosome missegregation in EB1- or APC-depleted cells. *EMBO J.*, **25**, 2814–2827.
30. Kikuchi,K., Niikura,Y., Kitagawa,K. and Kikuchi,A. (2010) Dishevelled, a Wnt signalling component, is involved in mitotic progression in cooperation with Plk1. *EMBO J.*, **29**, 3470–3483.
31. Kops,G.J., Weaver,B.A. and Cleveland,D.W. (2005) On the road to cancer: aneuploidy and the mitotic checkpoint. *Nat. Rev. Cancer*, **5**, 773–785.
32. Elowe,S., Dulla,K., Uldschmid,A., Li,X.L., Dou,Z. and Nigg,E.A. (2010) Uncoupling of the spindle-checkpoint and chromosome-congression functions of BubR1. *J. Cell Sci.*, **123**, 84–94.
33. Liu,X., Zheng,H. and Qu,C.K. (2012) Protein tyrosine phosphatase Shp2 (Ptpn11) plays an important role in maintenance of chromosome stability. *Cancer Res.*, **72**, 5296–5306.
34. Wu,K., Xie,D., Zou,Y., Zhang,T., Pong,R.C., Xiao,G., Fazli,L., Gleave,M., He,D., Boothman,D.A. *et al.* (2013) The mechanism of DAB2IP in chemoresistance of prostate cancer cells. *Clin. Cancer Res.*, **19**, 4740–4749.
35. Ahmed,A.A., Mills,A.D., Ibrahim,A.E., Temple,J., Blenkiron,C., Vias,M., Massie,C.E., Iyer,N.G., McGeoch,A., Crawford,R. *et al.* (2007) The extracellular matrix protein TGFBI induces microtubule stabilization and sensitizes ovarian cancers to paclitaxel. *Cancer Cell*, **12**, 514–527.
36. Seruga,B., Ocana,A. and Tannock,I.F. (2011) Drug resistance in metastatic castration-resistant prostate cancer. *Nat. Rev. Clin. Oncol.* **8**, 12–23.
37. Galsky,M.D. and Vogelzang,N.J. (2010) Docetaxel-based combination therapy for castration-resistant prostate cancer. *Ann. Oncol.*, **21**, 2135–2144.
38. Yamada,H.Y. and Gorbsky,G.J. (2006) Spindle checkpoint function and cellular sensitivity to antimitotic drugs. *Mol. Cancer Ther.*, **5**, 2963–2969.
39. Masuda,A., Maeno,K., Nakagawa,T., Saito,H. and Takahashi,T. (2003) Association between mitotic spindle checkpoint impairment and susceptibility to the induction of apoptosis by anti-microtubule agents in human lung cancers. *Am. J. Pathol.*, **163**, 1109–1116.
40. Sinnott,R., Winters,L., Larson,B., Mytsa,D., Taus,P., Cappell,K.M. and Whitehurst,A.W. (2014) Mechanisms promoting escape from mitotic stress-induced tumor cell death. *Cancer Res.*, **74**, 3857–3869.
41. Di Minin,G., Bellazzo,A., Dal Ferro,M., Chiaruttini,G., Nuzzo,S., Bicciato,S., Piazza,S., Rami,D., Bulla,R., Sommaggio,R. *et al.* (2014) Mutant p53 reprograms TNF signaling in cancer cells through interaction with the tumor suppressor DAB2IP. *Mol. Cell*, **56**, 617–629.
42. Petronczki,M., Lenart,P. and Peters,J.M. (2008) Polo on the rise - from mitotic entry to cytokinesis with Plk1. *Dev. Cell*, **14**, 646–659.
43. von Schubert,C., Cubizolles,F., Bracher,J.M., Sliedrecht,T., Kops,G.J.P.L. and Nigg,E.A. (2015) Plk1 and Mps1 cooperatively regulate the spindle assembly checkpoint in human cells. *Cell Rep.*, **12**, 66–78.
44. Wong,O.K. and Fang,G.W. (2007) Cdk1 phosphorylation of BubR1 controls spindle checkpoint arrest and Plk1-mediated formation of the 3F3/2 epitope. *J. Cell Biol.*, **179**, 611–617.
45. Liu,X.S., Song,B., Elzey,B.D., Ratliff,T.L., Konieczny,S.F., Cheng,L., Ahmad,N. and Liu,X.Q. (2011) Polo-like kinase 1 facilitates loss of Pten tumor suppressor-induced prostate cancer formation. *J. Biol. Chem.*, **286**, 35795–35800.
46. Zhang,Z., Hou,X.Z., Shao,C., Li,J.J., Cheng,J.X., Kuang,S.H., Ahmad,N., Ratliff,T. and Liu,X.Q. (2014) Plk1 Inhibition Enhances the Efficacy of Androgen Signaling Blockade in Castration-Resistant Prostate Cancer. *Cancer Res.*, **74**, 6635–6647.
47. Simizu,S. and Osada,H. (2000) Mutations in the Plk gene lead to instability of Plk protein in human tumour cell lines. *Nat. Cell Biol.*, **2**, 852–854.
48. Suijkerbuijk,S.J., van Osch,M.H., Bos,F.L., Hanks,S., Rahman,N. and Kops,G.J. (2010) Molecular causes for BUBR1 dysfunction in the human cancer predisposition syndrome mosaic variegated aneuploidy. *Cancer Res.*, **70**, 4891–4900.
49. Castedo,M., Perfettini,J.L., Roumier,T. and Kroemer,G. (2002) Cyclin-dependent kinase-1: Linking apoptosis to cell cycle and mitotic catastrophe. *Cell Death Differ.*, **9**, 1287–1293.
50. Cholewa,B.D., Liu,X. and Ahmad,N. (2013) The role of polo-like kinase 1 in carcinogenesis: cause or consequence? *Cancer Res.*, **73**, 6848–6855.
51. Strebhardt,K. (2010) Multifaceted polo-like kinases: drug targets and antitargets for cancer therapy. *Nat. Rev. Drug Discov.*, **9**, 643–660.